Environmental Advances 18 (2024) 100600

Contents lists available at ScienceDirect

Environmental Advances

journal homepage: www.sciencedirect.com/journal/environmental-advances

Phi6 virus transmission in Arctic outdoor air and the effects of solar UV radiation on virus and host viability

Rasmus Malmgren[a,*], Svetlana Sofieva-Rios[a,b], Kaisa Lakkala[b,c], Eija Asmi[b], Yan Sun[d], Michael Todt[b], Paavo Heikkilä[e], Dennis Bamford[a], Martin Romantschuk[a,d], Nina Atanasova[b,a]

[a] University of Helsinki, Molecular and Integrative Biosciences Research Programme (MIBS), Faculty of Biological and Environmental Sciences, Viikinkaari 9 00720, Helsinki, Finland
[b] Finnish Meteorological Institute, Climate Research Programme, Erik Palménin aukio 1 00560, Helsinki, Finland
[c] Finnish Meteorological Institute, Space and Earth Observation Centre, Tähteläntie 62 99600, Sodankylä, Finland
[d] University of Helsinki, Ecosystems and Environment Research Programme, Faculty of Biological and Environmental Sciences, Niemenkatu 73 15140, Lahti, Finland
[e] Aerosol Physics Laboratory, Physics Unit, Faculty of Engineering and Natural Sciences, Tampere University, Korkeakoulunkatu 3 33720, Tampere, Finland

A R T I C L E I N F O

Keywords:
Environmental virology
Environmental microbiology
Aerovirology
aerosol
Ultraviolet radiation
Aerosol transmission

A B S T R A C T

Virus seasonality is affected by many environmental factors. UV radiation is a less studied but potentially important factor in virus outdoor aerosol transmission. Virus aerosol transmission in an Arctic environment was simulated by nebulizing Phi6 outdoors to study longer range (0-75 m) transmission. Aerosolized viruses were collected using host-containing agar plates, Biosamplers and filter collectors. Additionally, the effects of long-term exposure to solar UV radiation were studied on Phi6 and its host bacteria *Pseudomonas phaseolicola.* Phi6 remained infectious in aerosols for at least 50 m outdoors, however, potential for longer transmission distance still exists. Exposure to solar UV radiation did not significantly affect Phi6 viability, however, a decreasing trend was seen over an 8 h exposure time. Potential UV radiation related damages were found in the host bacteria's genome, but not in Phi6. This study shows that some viruses can remain infectious and travel for relatively long distances outdoors. Solar UV radiation was found to have minimal or no effect on Phi6 aerosol transmission at these distances, however, Phi6 is known to be resilient against UV radiation. Further studies are required with longer distance collection to understand the full potential of virus aerosol transmission outdoors. Additionally, other model viruses should be experimented with to understand how different viruses remain infectious in aerosols.

1. Introduction

Respiratory viruses cause up to a billion infections yearly (WHO 2024 a-b, 2023), making them a major influence in global health and economy (Courville et al 2022). The recent SARS-CoV-2 pandemic urged multiple studies on aerosol transmission of these viruses both indoors and outdoors (Dinoi et al. 2022), however, long distance transmission remains poorly studied. Previously, only avian influenza has been shown to remain infectious for up to 70 meters, however, aided by exhausted air (Torremorell et al., 2016).

Respiratory virus infections are commonly known to be seasonal. The seasonality of airborne virus infections is affected by many environmental factors, such as temperature, humidity (Sajadi et al 2020), and air pollutants (Groulx et al 2018). Solar ultraviolet radiation (UVR), however, is a much less studied, but potentially important factor in virus seasonality (Carvalho et al 2021; Guasp et al 2020). UVR is divided into three bands according to its wavelength, with UV-C including the shortest (200–280 nm), UV-B medium (280–315 nm), and UV-A the longest wavelengths (315–400 nm). UV-C and UV-B radiation induce the formation of cyclobutane pyrimidine dimers and pyrimidine-6, 4-pyrimidone photoproducts in DNA by forming covalent bonds at di-pyrimidine sites, leading to DNA breakage and replication arrest (Rastogi et al 2010). While UV-A induces these changes at di-pyrimidine sites at a lower rate, it can also promote mutations in other parts of DNA by forming reactive oxygen species (Mullenders 2018). The effects of UV radiation on RNA resemble those on DNA, with the addition of uridine and cytidine hydrate formation (Singer 1971). Additionally, viruses tend to be more susceptible to shorter wavelengths of UVR (Ma et al., 2021). UV-C also promotes site-specific self-cleavage in viral RNA (Ariza-Mateos et al., 2012). Furthermore, viruses with a single-stranded

* Corresponding author

https://doi.org/10.1016/j.envadv.2024.100600
Received 20 May 2024; Received in revised form 22 October 2024; Accepted 11 November 2024
Available online 12 November 2024

genome are more susceptible to UVR induced genomic damage (Qiao et al., 2018), while those with shorter genomes are better protected from it (Rodriguez et al., 2014).

The spectrum of solar UV that reaches Earth's surface differs from that of germicidal UV lamps. The Earth's ozone layer absorbs UV-C radiation completely and the UV-B wavelengths of the solar spectrum partially, leaving only UV-A and some UV-B radiation reaching Earth's surface (Lubin & Jensen 1995). Germicidal UV lamps, or monochromatic lamps, usually emit only UV-C radiation at a specific wavelength, most commonly at 254 nm, which is close to the wavelength of DNA's peak absorption. The lack of UV-C and part of UV-B in surficial solar UV spectrum makes viruses less sensitive to solar UV than to germicidal lamp, requiring longer exposure times under solar UV for significant viral inactivation (Weyersberg et al., 2022). While UVR inactivation of viruses is well-studied (Carvalho et al 2021; Rockey et al 2021), the effects of solar UVR on aerosolized viruses remain poorly studied.

The aim of this study was to measure longer distance (0-75 m) virus aerosol transmission and short-term effects of solar UVR on virus inactivation. Phi6 was used as a model virus to study enveloped virus aerosol transmission as it is harmless to humans and the environment, requires no biosafety precautions, and is a commonly used model virus for aerosol transmission of respiratory viruses such as influenza and coronaviruses (Oksanen et al 2022; Turgeon 2014). Previous research has demonstrated that Phi6 is relatively resilient to UV radiation (Ma et al 2021; Weyersberg et al. 2022). Here we experiment this resilience towards solar UVR in a natural outdoor environment combined with the potential for long distance aerosol transmission. Solar UVR spectrum is highly specific and difficult to reproduce *in vitro* indicating the importance of experimental research in real outdoor environments.

2. Materials and methods

2.1. Description of the research site

Exposure tests and field simulations were conducted at the Finnish Meteorological Institute Arctic Space Centre in Sodankylä (67°N, 23°E). The Centre is a research station where infrastructure enables multidisciplinary laboratory and field simulations by offering versatile measurements of weather and atmosphere. The site is 7 km south of the Sodankylä village near the river Kitinen. The surrounding area is characterized by pine forest and swamp. In June, the temperature range is typically from +5°C to +20°C, and the weather is continental. In June, the minimum solar zenith angle (SZA) is around 45°, and the sun is almost constantly above the horizon due to the location being north of the Arctic circle.

The field simulations were conducted at the test field around one of the satellite antennas near the sounding station. The field was a 100×200 m^2 open area surrounded by pine forest (Supp. Fig. 3). A test automatic weather station (AWS) and a test mast measuring wind, temperature and relative humidity were in the field.

UV exposure tests were conducted in both the measurement platform of the sounding station and in the optical laboratory of the site (Lakkala et al., 2016). The measurement platform has several solar radiation measurements which routinely measure global radiation, UV radiation and total ozone. The horizon is free from trees until around SZA 80°. Meteorological data were obtained from the official AWS of the site, next to the sounding station (World Meteorological Organization site code 02836). Control samples were kept out of UV exposure in a synoptic station weather box in outdoor conditions next to the AWS and the sounding station.

2.2. Meteorological data

Temperature, relative humidity, wind speed, direction, and gusts were downloaded from the official AWS via FMI's database as 1 minute data for outdoor UV exposure tests. For outdoor simulations, similar meteorological parameters were downloaded from two FMI's test weather stations. Each time, the weather station located closest to the simulation was chosen. PT100- (Pentonics AB, Sweden) and HMP155D-sensors (Vaisala Oyj, Finland) were used to monitor temperature and humidity respectively. The wind speed and wind direction data were recorded as one- or ten-minute averages with an acoustic anemometer UA2D (Adolf Thies GMBH & CO.KG, Germany). Thermochron data loggers were used to continuously monitor the temperature next to the nebulizer, at 5 m in three directions and at 30 m downwind. A Thermochron data logger was also placed in the weather box together with the control samples. The temperature next to the virus and bacteria samples was monitored on the measurement platform using a Hanna Checktemp pocket thermometer model HI 98501.

2.3. UV measurements

2.3.1. Outdoor measurements

Two Brewer spectroradiometers, Brewer#037 and Brewer#214, measured UV radiation at the measurement platform of the sounding station. Their measurement schedule included both total ozone measurements and UV scans. During the field simulations and UV exposure tests, the #214 was optimized to measure several UV scans in a row. The Brewer is a scanning spectroradiometer with a wavelength range of 290 nm to 325 nm (Brewer#037) or to 363 nm (Brewer#214). The #037 is a single monochromator and the #214 a double monochromator device. They measure incoming global radiation on a horizontal surface. The UV irradiance is recorded at 0.5 nm steps, and the whole scanning time is 3 to 5 minutes. The irradiance scale is traceable to PTB through the national metrological institute MIKES Aalto, and the post-processing of the data includes correction for all known errors (Lakkala et al. 2008; Mäkelä et al. 2016). Both Brewers are compared against the world reference QASUME every 4 years and have shown good stability and difference less than 6 % compared to QASUME at wavelengths longer than 305 nm.

Two GUV multichannel radiometers (Biospherical Instrument Inc., United States) were also used for measurements on the platform next to the spectroradiometers. The GUVs are the same that are used for Antarctic UV measurements in the Marambio station (Lakkala et al. 2020). The GUV radiometer has five UV channels, with a bandwidth of about 10 nm and center wavelengths at 305, 313, 320, 340, and 380 nm. It also has a channel measuring visible radiation at 555 nm and one measuring the photosynthetically active radiation (PAR). The GUVs are regularly calibrated at Biospherical Instruments Inc. and compared against the spectroradiometers in Sodankylä. The difference between both GUVs and the Brewer#214 was less than 6 % at SZAs smaller than 60° on June 4th, 2021.

The one-minute dose rate data from the GUV radiometers were used to calculate UV doses for selected UV exposure time periods and for field simulations. The DNA damage weighting of DNA damage dose rates of the GUV is directly provided by Biospherical Instruments (Bernhard et al., 2008) and available at https://gml.noaa.gov/grad/antuv/docs/version2/doserates.SetlowBSI.txt (last visited 15 Feb 2024). This weighting is a parametrization of the action spectrum described by Setlow (1974). In some of the UV exposure experiments, a filter blocking the UVB wavelengths (polyester filter) of the solar spectrum was used. As we had two GUV radiometers, the diffuser of one GUV was covered by a UVB blocking filter, while the other remained uncovered, allowing short UVB wavelengths to pass through the diffuser.

2.3.2. Laboratory experiments

A 1 kW tungsten-filament incandescent halogen lamp of type DXW was used to expose samples to UV radiation in the laboratory. The same setup as for the calibration of the Brewer spectroradiometer was used, which is explained in detail by Lakkala et al. (2016). The UV-lamp was operated horizontally with a vertical optical axis at 50 cm from the sample. The lamp emits UVC, UVB, UVA, and near infrared radiation, and its spectrum is shown compared to a measured solar midday UV spectrum in Fig. 1. The room temperature was kept constant at 23°C, and the temperature of the sample was recorded before and after exposure. For the calculation of UV doses received by UV samples in the laboratory, the Setlow (1974) DNA damage spectrum was parameterized following Bernhard et al. (1997) and normalized to 254nm.

2.4. Viruses, microbial strains, and growth media

Pseudomonas syringae pathovar phaseolicola HB10Y (HB10Y) was used as the host for Phi6. The bacteria were grown in Luria-Bertani-Lennox (LB)-broth containing 0.5 % NaCl at RT (22°C) with aeration overnight. *P. syringae* and Phi6 were originally obtained from Ann Vidaver, University of Nebraska (Vidaver et al., 1973). Agar plates containing HB10Y (HB10Y plate) were prepared by mixing 100 µl of bacteria grown overnight with 3 ml LB-soft agar and pouring it on LB-agar plates. HB10Y plates were used to collect naturally depositing aerosols, without external pumps.

Phi6 was purified using the sucrose gradient method described by Bamford et al. (1995). Purified virus was used in all UV exposure assays as well as outdoor transmission measurements. Phi6 solutions were prepared by mixing purified Phi6 (~$1•10^{14}$pfu/ml) with 20 mM K-phosphate for a final concentration of $1•10^{11}$ pfu/ml for aerosolization and $1•10^{10}$ pfu/ml for UV tests.

2.5. Aerosol particle measurements

Aerosol particle number concentration at >10 nm range was measured by a TSI hand-held Condensation Particle Counter (CPC) model 3007 (TSI Inc., USA). The CPC data during experiments were logged at 1s time resolution. The CPC volumetric flowrate (0.7 LPM) was measured before and after the experiment with a flow calibrator (Gilian Gilibrator-2, Sensodyne) and the total concentration was compared to a reference laboratory CPC (TSI model 3772) and corrected accordingly.

Aerosol particle number size distribution was measured by two different techniques: Aerodynamic Particle Sizer (APS) model 3321 (TSI Inc., USA) and Optical Particle Sizer (OPS) model 3330 (TSI Inc., USA). The APS measurement range is from ~500 nm to 20 µm (aerodynamic equivalent diameter), divided into 52 logarithmically spaced channels. APS data were recorded at 1-min time resolution. The OPS measurement range is from ~300 nm to 10 µm (optical equivalent diameter) divided into 16 logarithmically spaced channels. OPS data were recorded at 10 s time resolution. The flow rate of APS and OPS were 5 LPM and 1 LPM respectively, which were verified prior to, and after, the campaign.

A Wideband Integrated Bioaerosol Sensor (WIBS-NEO, Droplet Measurement Technologies Inc., USA) was used to measure the biogenic background of aerosol particles by single-particle fluorescence spectroscopy. It utilizes two excitation wavelengths (280 nm and 370 nm) and two emission detection channels (310–400 nm and 420–650 nm). Utilizing the different wavelength combinations, 3 main fluorescence channels (A: ex.: 280 nm, em.: 310–400 nm; B: ex. 280 nm, em.: 420–650 nm; C: ex.: 370 nm, em.: 420–650 nm) and their combination channels (A+B, A+C, B+C, A+B+C) can be constructed to enhance the resolution power between different fluorescent particle species (Savage et al. 2017). Additionally, WIBS measures the optical aerosol size distribution and shape factor of individual particles. WIBS measures the aerosol in real time with a flow rate of 0.3 LPM and a maximum sampling rate of 13 particles/s for the fluorescence analysis.

The aerosols were sampled at atmospheric humidity. Background subtraction of naturally occurring atmospheric aerosol was carried out for each instrument based on measurement ~30 minutes prior to and ~30 min following virus collection for each experiment. For the OPS and APS, background in each size channel was treated individually. For OPS and APS size bins below 1 µm in diameter, and CPC data, a linear trendline was fit to background data and subtracted directly from experimental data. For OPS and APS size bins larger than 1 µm, where concentrations are generally low, the median value for the background period was subtracted from experimental data. There are exceptions to this method, which are noted where applicable.

The APS, CPC, and WIBS were placed 3 m downwind, and the OPS 7.5 m downwind, from the nebulizer. All aerosol measurement devices' inlets were at the altitude of the virus source.

2.6. Outdoor virus simulations

2.6.1. Setup

The final setup used in the experiments in Sodankylä was derived from the feasibility test setups (Supp. 1). 1.5 m high wooden stands (Supp. Fig. 4) were built to hold HB10Y plates at the height of the output of the nebulizer. The stands were placed in three directions: downwind, and 90° to the left and right, according to the preliminary tests. Three replicate HB10Y plates were placed on the stands at 1 m, 3 m, 5 m, 7.5 m, 10 m, 15 m, 20 m, 25 m, 30 m, 40 m, 50 m, 60 m, and 75 m,

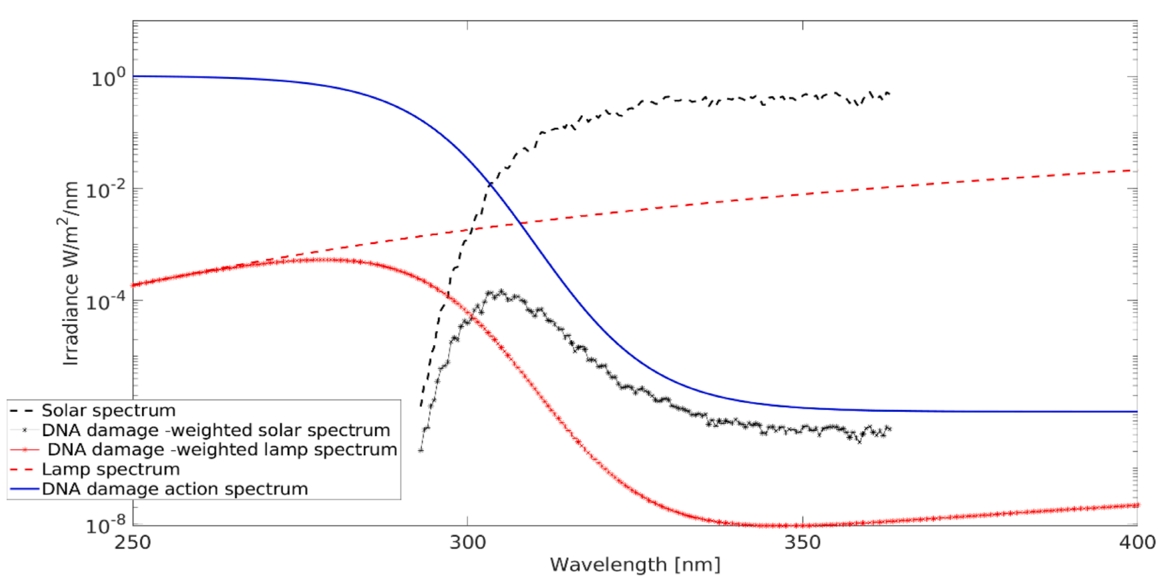

Fig. 1. Solar midday spectrum (SZA 45°) on June 4th, 2021, and the spectrum of the UV lamp used in the study. The plot also includes both spectra weighted by the DNA damage action spectrum. The DNA damage action spectrum normalized to 254 nm is also plotted. Note the logarithmic scale.

downwind, and 1 m, 3 m, 5 m and 10 m to the left and right. The setup was adjusted according to the main wind direction. The meteorological factors were monitored as stated above. An Omron compare Pro C900-nebulizer was used to aerosolize Phi6 solution at ~0.4 mLPM for 30 min.

2.6.2. Virus transmission

Virus transmission was studied using HB10Y plates, 5 ml Bio-samplers (SKC) and a prototype filter collector (Supp. Fig. 5-6). HB10Y plates were used as passive collectors to collect naturally depositing aerosols, while the Biosamplers and filter collectors collected actively, using a pump. Two Biosamplers filled with 5 ml of HEPES were operated with an airflow of 12.5 LPM. Polycarbonate (PC) and cellulose-acetate (CA) filters were used in the filter collector, and their pumps were operated at a flow of 5 LPM. Controls were taken right before and 30 min after the experiments by leaving three HB10Y plates open on the stands downwind for 30 min.

2.6.3. UV assay on virus infectivity

Phi6 solution was pipetted and dried onto empty plastic Petri dishes in a laminar hood. The dried droplets were exposed to a UV-lamp, or solar UV. A weather box was used as a control environment for solar UV, as it is impermeable for UV from outside but matches other environmental parameters. Control samples for the UV-lamp were kept in the same room with the UV-lamp to ensure similar environmental factors. The dried droplets were subjected to UV for up to 2 h under the UV lamp and up to 8 h under solar UV. Outdoors, the Petri dishes containing the dried droplets were placed on the measurement platform. Ice packs were placed under the Petri dishes to prevent the samples from heating.

To study the effects of UVA on the viruses outdoors, the droplets were covered with UVC and UVB blocking polyester filters. In the laboratory, alternatively to the polyester filters, cellulose diacetate filters were used to block only the UVC wavelengths of the lamp spectrum. In the laboratory, the filters were set up on the lowermost baffle (see Fig. 2 in Lakkala et al. 2016) of the measurement setup. The effect of the filter on the irradiance of the lamp can be seen in Supp. Fig. 7.

2.7. UV assay on cell viability

HB10Y UV sensitivity was studied using replica plating technique (Lederberg & Lederberg, 1952) for creating multiple plates with comparable colonies. HB10Y overnight inoculate was plated in dilutions from 10^{-2} to 10^{-8} to produce a plate with optimal amount of single, distinguishable colonies for replicating, and incubated overnight at room temperature. After the optimal dilution was selected (dilution 10^{-7}), a replicating apparatus with sterile velvet cloth was pressed to the plate surface and then moved and pressed onto five fresh LB-Lennox plates. The plates were incubated overnight at room temperature. The replicate plates were used to produce triplicates using replica plating. The plates were then exposed to UVR as described above. Controls were kept in the weather box described above.

After the UV exposure, replica plates were incubated at RT overnight allowing the survived cells to proliferate. On the following day, bacterial cells were collected with 0.5 ml of HEPES buffer from the agar surface into Eppendorf-tubes, snap-frozen in liquid nitrogen and stored at -80 °C until analysis.

Once defrosted, the samples were mixed briefly using vortex and the cell density (A_{600}) was measured with Nanodrop using sterile cuvettes. The absorbance was measured for 200 μl of bacterial samples.

2.8. Nucleic acid extraction

RNA extraction for Phi6-samples was done using QIAamp Viral RNA Mini Kit, following the kit protocol. Prior to extraction, 6.16 ml of AVL-buffer and 61.6 μl of carrier-RNA-AVE-buffer were prepared afresh. RNA samples were eluted into 60 μl of RNase-free water. RNA concentrations and the purity of extracted RNA were assessed with Nanodrop (Thermo Scientific, USA), results shown in Supp. Tab. 1.

DNA extraction was done according to Sofiev et al. (2022) using only lysozyme instead of the enzyme mix, and 600 μl of each sample. Quality and quantity of the extracted DNA was assessed using Nanodrop shown in Supp Tab 2.

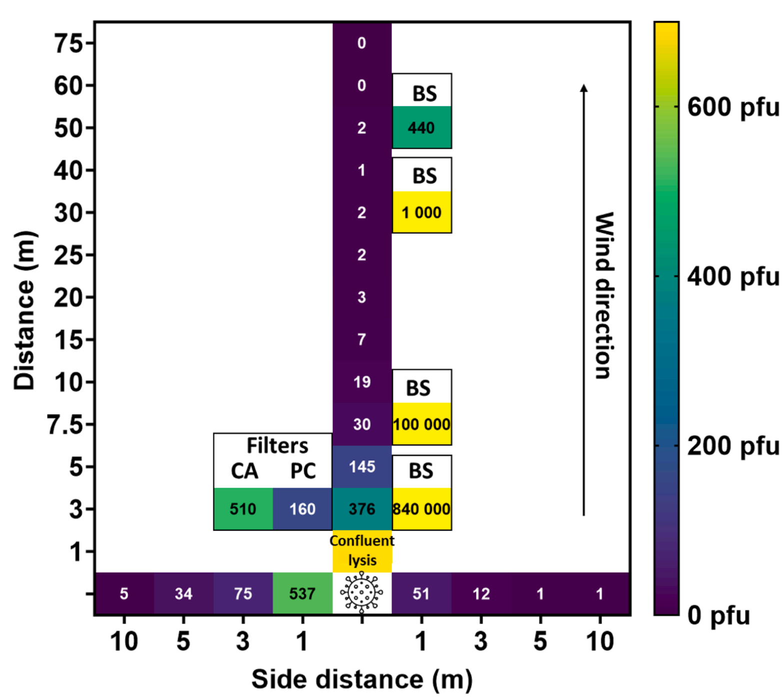

Fig. 2. Infective virus counts in field simulations after 30 min of nebulization. Biosamplers (BS) and the filter collector were situated at 0 m side distance. Values presented are averages of all measurements rounded up to the nearest unit.

2.9. Sequencing and sequence analysis

Phi6 samples with exposure to the highest amount of UVR were chosen for sequencing. No replication round was performed for the virus samples. For HB10Y, samples were sequenced from one growing and three non-growing colonies after UVR exposure. Non UVR exposed controls were sequenced alongside both Phi6 and HB10Y.

The extracted RNA was reverse transcribed to cDNA prior to sequencing. The cDNA and DNA samples were sequenced using the Illumina MiSEQ next generation sequencing platform. Adapters were clipped and the reads were trimmed using Trimmomatic. The trimmed reads were assembled into contigs de novo with Spades (Prijbelski et al., 2020) and then sorted against reference genomes obtained from NCBI Genome database with Burrows-Wheeler Alignment Tool (BWA).

Using Varscan v.2.4.3 (Koboldt et al., 2012), the variants present in the genomes of HB10Y samples RP1-5 were identified and variants deviating from those found in RP5. The Phi6 sample genomes were scanned with INDELseek (Au et al., 2017) for potential rupture points visible as deletions in the genome data. The variants and deletions found in samples were visualized with Geneious Prime 2023.2 (https://www.geneious.com). Annotations for the reference sequences were acquired from NCBI Genome database (access codes: HB10Y: GCF_001294035.1; Phi6: NC_003715, NC_003716, NC_00371).

2.10. Statistical analysis

Statistical analyses were performed using GraphPad Prism 10.1.2. Correlations were calculated using the two-tailed Pearson correlation test.

3. Results

3.1. Field aerosol transmission simulations

Infective viruses were collected up to 50 m downwind from the nebulizer with HB10Y plates in three separate simulations, as well as with Biosamplers in one simulation. HB10Y plates beyond 50 m collected no viruses and Biosamplers were not placed further away. Virus numbers collected with HB10Y plates and Biosamplers were high at close proximity but diminished exponentially further from the source. After 20 m, consistently fewer than 5 viruses were detected on HB10Y plates, however, viruses were still detected on most plates (Fig. 2). Markedly more viruses were detected with Biosamplers compared to HB10Y plates (Fig. 2). The CA-filter collected three times more infectious viruses compared to the PC-filter, however the Biosamplers proved to be much more efficient, collecting over 1600-fold more than the CA-filter (Fig. 2). Control plates exposed before, and 30 min after the phage release, were consistently free from plaques, confirming the absence of background viruses.

Wind direction played a major role in the transmission of viruses, but wind speed was not found to significantly correlate with virus detections on HB10Y plates (P=0.81 at 50 m; P=0.38 at 30 m). Wind directions and speeds are presented in Supp. Tab. 8. Similarly, the level of UV-radiation outdoors during the tests were not observed to affect virus infectivity in 30 min simulations.

3.2. Aerosol measurements

Fig. 3 shows the mean CPC, OPS and APS aerosol concentration enhancement due to the nebulizer during 30 minutes of sample collection.

Fig. 4 shows the mean aerosol size distribution for the background period before and after each experiment, and during each experiment, measured by APS. Elevated aerosol concentrations in size range >0.5 μm were observed for 3 out of 5 experiments where APS data is available. In the simulation without elevated aerosol concentration, wind direction was not optimal for the setup.

With the WIBS, an increase in fluorescent particle count was evident when comparing the background and simulation situations. The increase was notably visible in particle sizes > 1 μm in diameter and in channel A, which has been associated with microbial fluorescence in previous studies as well (Savage 2017). Fig. 5 shows the results for all the simulations with a comparison to the background aerosol, measured within 1 hour of the simulation.

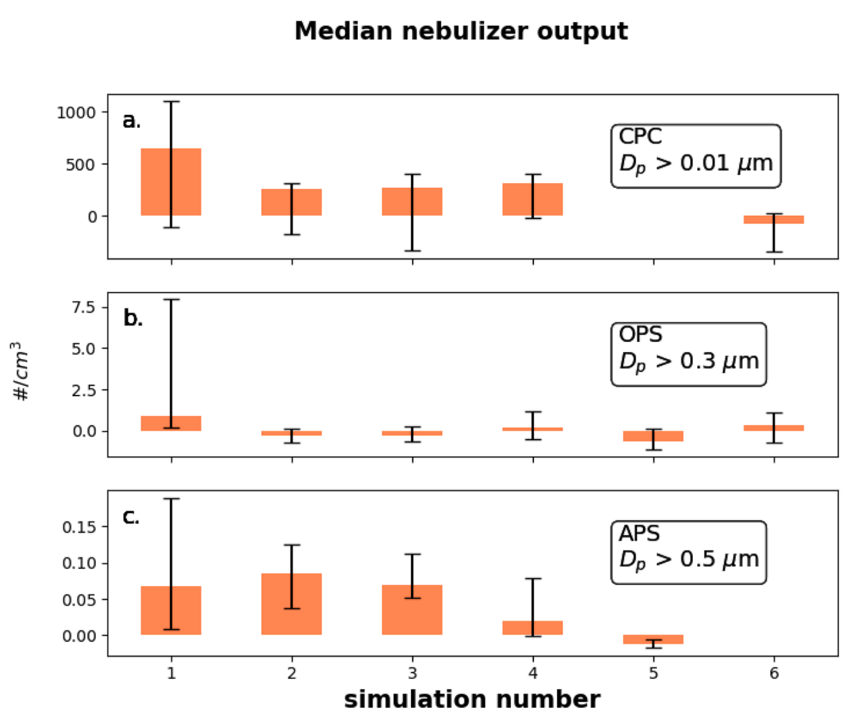

Fig. 3. Median total aerosol number concentration, as measured by CPC (a), OPS (b), and APS (c) at size range >0.01 μm, >0.3 μm and >0.5 μm, respectively. Error bars show the interquartile range.

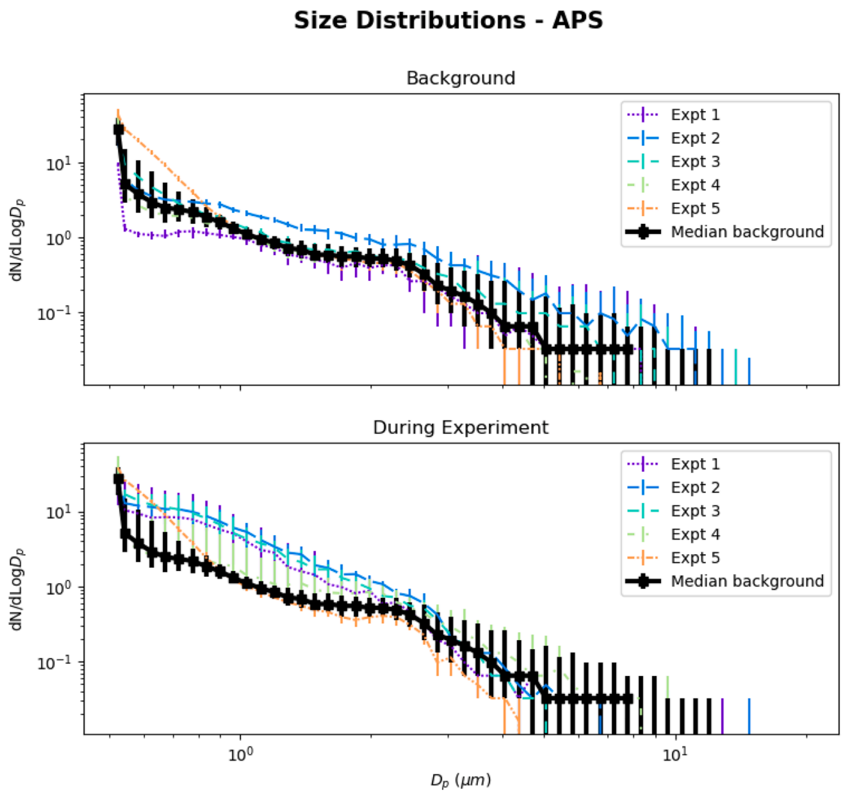

Fig. 4. Median aerosol size distributions measured by APS, with error bars showing interquartile range for experiments 1-5 (colored lines), and the median of all background times (solid black). Size distributions for five of six experiments at Sodankylä were compared to the same median background profile (black line). APS data from experiment 6 is missing due to equipment failure.

3.3. UVR exposure experiments

While no statistically significant differences were observed between the control and solar UVR exposed samples, a decreasing trend in virus concentration of exposed samples could be seen (Fig. 6). A significant (p=0.0472) correlation was found between unweighted solar UVR dose and virus concentration decrease; however, not with the DNA damage weighted UV dose. Blocking UVB seemed to slow down the decrease only slightly. Similarly, when exposed to UVR under a UV lamp, the UVB+UVA, and UVA exposed samples showed similar decreases in infectious virus concentration. Exposure to the full spectrum led to a more pronounced decrease (Fig. 7).

3.4. UV measurements

The campaign week was sunny with several mostly cloudless days. The daily maximum UV index of 4 was reached each day around solar midday. One minute data of UV index, UVB, UVA and PAR radiation are shown in Fig. 8 for the whole campaign. The high variability in solar radiation measurements, observed for example during June 5th, is due to rapidly moving cloudiness which is typical for the site.

3.5. Genome mutation analysis

In Phi6 genomes, eight two-base deletion-like damages were identified, however, none of these were exclusive to the UVR exposed samples. All but one of these mutations occurred in the M segment (Fig. 9). Three of these deletions were found in the P3 protein coding area and one in the P5 protein coding area. The remaining four were in non-coding areas (Supp. Tab. 5). No replication rounds were performed to verify the damages as mutations.

We identified 6 recurrent SNPs found in all non-growing HB10Y sample genomes but not the growing sample genomes. One additional SNP and one two-base substitution were also found in 80 % of the non-growing genomes. Out of these mutations, three were transversions of purine to pyrimidine: two common to all and one common to 80 % of the sequences of non-growing genomes. All detected mutations were found in non-coding regions of the genome (Supp. Tab. 6).

4. Discussion

Bacteriophage Phi6 was employed here to investigate airborne virus transmission in Arctic outdoor air. The effect of solar UVR on virus and host cell viability was also studied in a laboratory. In a simulation first of its kind, infectious viruses were detected outdoors up to 50 m away from the source with two different collection methods: deposition on host-containing agar plates (HB10Y plates) and collection with Biosamplers. The observed quantity of viruses collected by Biosamplers suggests a potential for even longer distance detection of infective viruses.

Biosamplers collected on average 500 and 220 times more infectious viruses at 30 and 50 m respectively, compared to HB10Y plates (Fig. 2). These findings indicate that even though no viruses were observed on HB10Y plates after 50 m, they could still potentially be detected using Biosamplers. Moreover, this is supported by the fact that detected virus counts with Biosamplers were only halved from 30 m to 50 m. Calculating linear regression from these two Biosampler points suggests that detection would be possible for up to 65 m. Biosamplers were placed furthest at 50 m in this study, however, these suggestions agree with previous findings from poultry farms (Torremorell et al., 2016). Aerosol samplers should also be tested to determine the most suitable detector for outdoor samples. In addition to remaining infectious for at least 50 m downwind, infectious viruses were found at least 10 m from the source to the sides. As with downwind, longer distance detection using Biosamplers would provide a fuller view of virus transmission through aerosols. Further studies with longer distance collection using

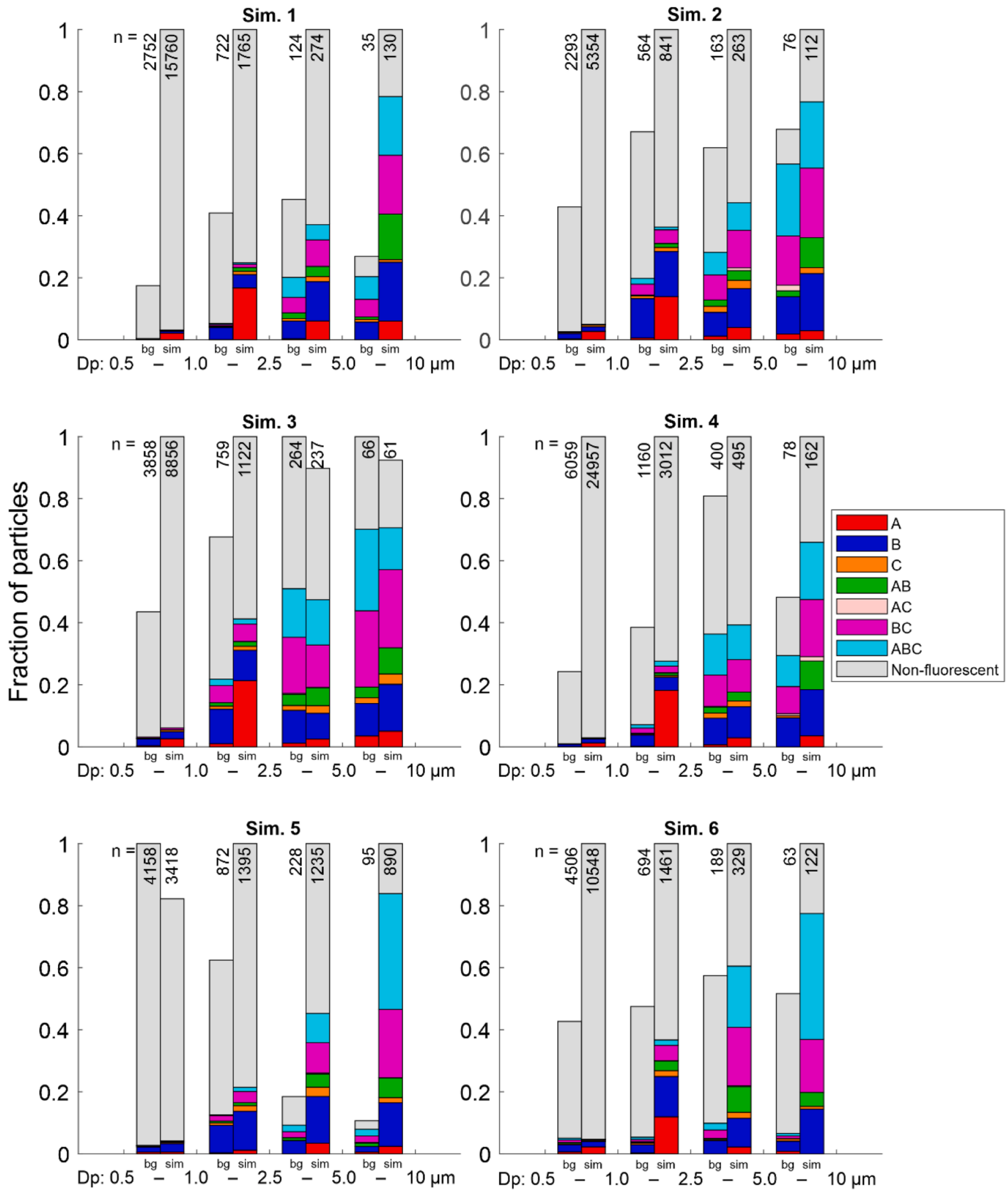

Fig. 5. Comparison of fluorescent particles in the background and simulation as a function of particle size. The particle size limits are 0.5–1.0 µm, 1.0–2.5 µm, 2.5–5.0 µm, and 5.0–10 µm. The background is the left stack bar of the pair, and the simulation is the right. Different fluorescent channels are denoted with different colors and the height of the segment reflects the number of particles detected in the corresponding channel. Each pair of bars have been normalized with the higher number of particles in the corresponding size range. As can be seen from the figure, most simulations are seen as an increase in the total and fluorescent particles especially in the larger particle sizes and in channel A. In a few cases (e.g. size range 0.5–1.0 µm of sim. 210607) the simulation cannot be distinguished from the background. The total number of measured particles during the data collection period is shown at the top of the bars. The data collection time may vary slightly depending on the simulation, and thus the total number count is not inter-comparable between simulations.

Biosamplers are needed to understand the maximum distance viruses can remain infectious in outdoor air.

Biosamplers were found to be the best collection method for infectious viruses from the air compared to deposition plates and filter collectors. With Biosamplers, compared to HB10Y plates, we were able to collect an over 1000-fold number of infectious viruses at short distances (5 m and 10 m) and 100-fold at longer distances (30 m and 50 m) (Fig. 2). The cellulose-acetate filter was found to be better in preserving virus infectivity than the polycarbonate filter. Neither of the filters were as efficient as HB10Y plates or Biosamplers, however. Additionally, the number of viruses detected with the filter collector was inconsistent compared to other collection methods. Low infectious virus counts on the filters is likely due to inactivation from dehydration during sampling (Tseng & Li 2005).

While air dilution undoubtedly has a major effect on virus detection at longer, above 10 m distances, its effect compared to virus inactivation from eg. dehydration is difficult to assess without data on total virus particles. Approximately $1.2{\cdot}10^{12}$ pfu of Phi6 were nebulized during each simulation, while on average $8.4{\cdot}10^{5}$ pfu were recovered at 3 m using a Biosampler. Furthermore, at 7.5 m $1{\cdot}10^{5}$ pfu were detected, suggesting that a large portion of viruses are inactivated already during nebulization. For future studies, collecting samples for qPCR analysis is advised to understand what portions of this reduction are due to virus inactivation and air dilution.

Phi6 is known to be comparatively resilient against UVR (Ma et al., 2021; Weyersberg et al., 2022). Solar UVR was found to have minimal effect on Phi6 infectivity in the Arctic environment in our dry droplet tests. A 0.5 log reduction in infectious viruses, compared to the control,

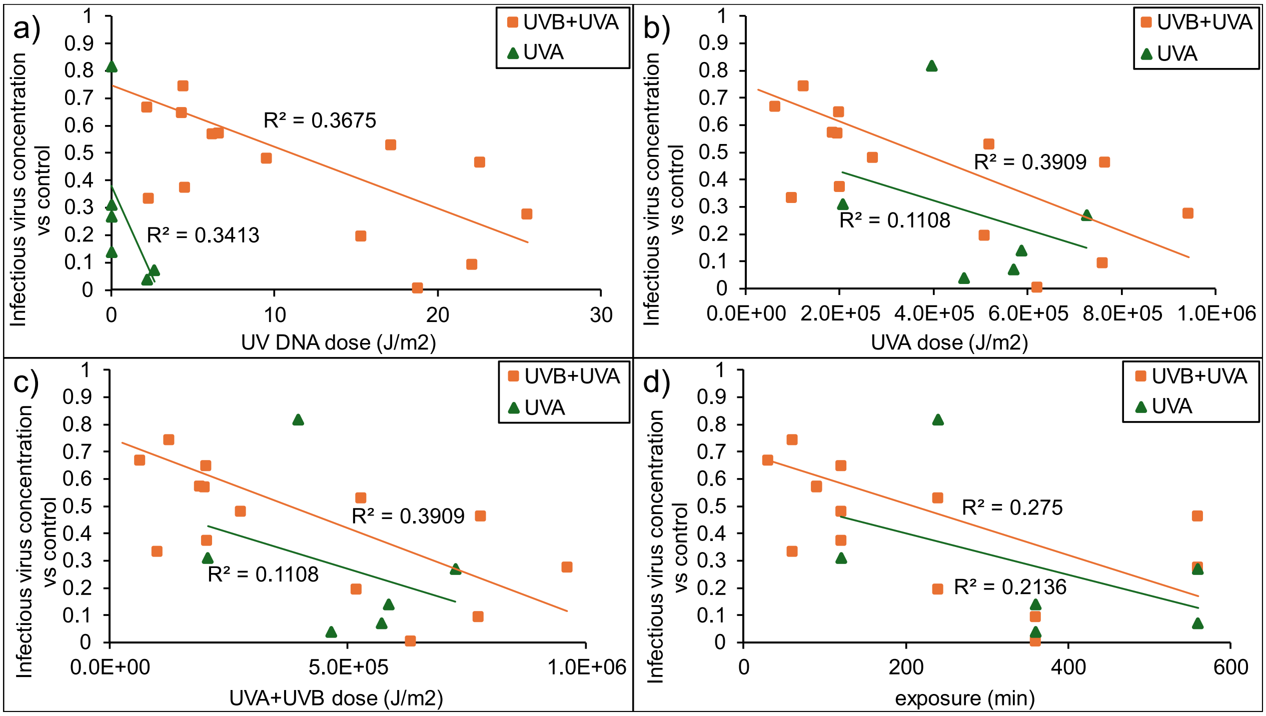

Fig. 6. Recovered infectious virus concentrations after exposure to solar UVR in proportion to the control on a) DNA damage–weighted UV doses (254 nm), b) non-weighted UVA dose, c) non-weighted UV dose (including both UVB and UVA) and d) exposure time. The legend labels signify the UVR spectra samples were exposed to.

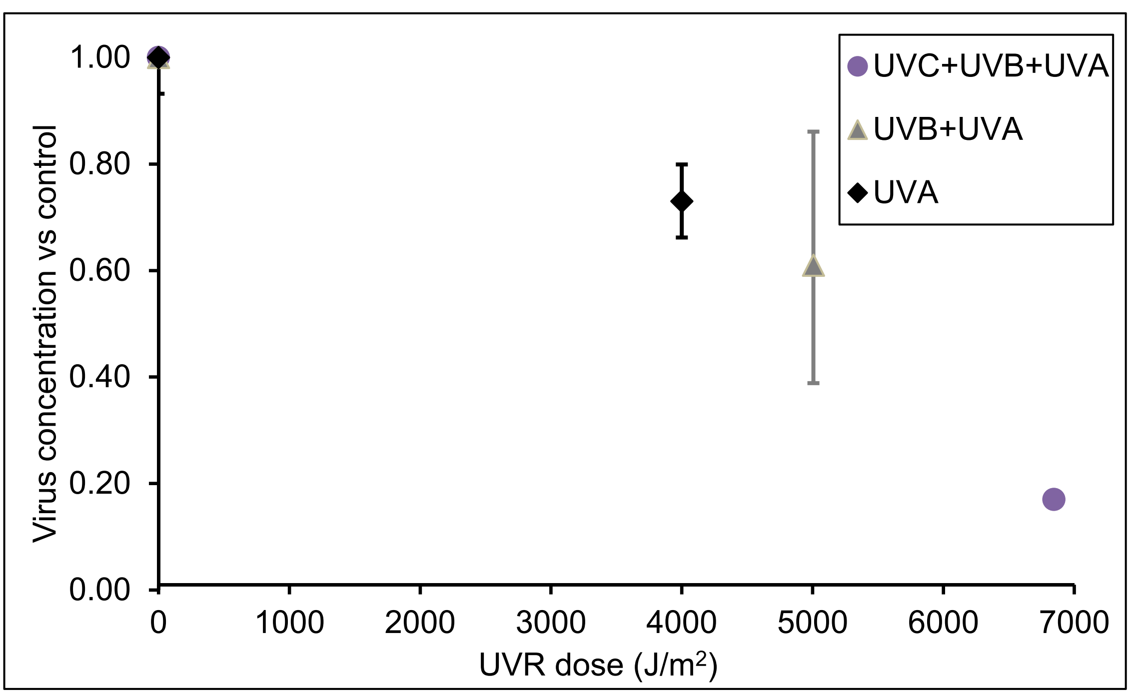

Fig. 7. Recovered infectious virus concentrations relative to control after 120 min exposure under UV lamp.

was seen after 2 h exposure, with the highest reduction of 2 logs being at 4 h. Phi6 UVR resilience could be partly explained by the high virus concentration used in the experiments, which has been found to conserve virus infectivity (Bangiyev et al., 2021). The structure of phage capsids has been suggested to be responsible for higher UVR tolerance of virus particles by Plano et al. (2021). Recent study comparing the UVR susceptibility of Phi6 and SARS-CoV-2 supported this theory concluding that though Phi6 is similar in size and outer membrane structure, Phi6 requires much higher dose of UVR for virus aerosols to lose infectivity (Weyersberg et al 2022). Though no statistically significant differences were detected in virus infectivity compared to the controls, a decreasing trend could be seen (Fig. 6). Although different UV lamps cannot be fully compared due to differences in their spectra, similar decreases in infectious Phi6 concentration with similar UV doses have been reported

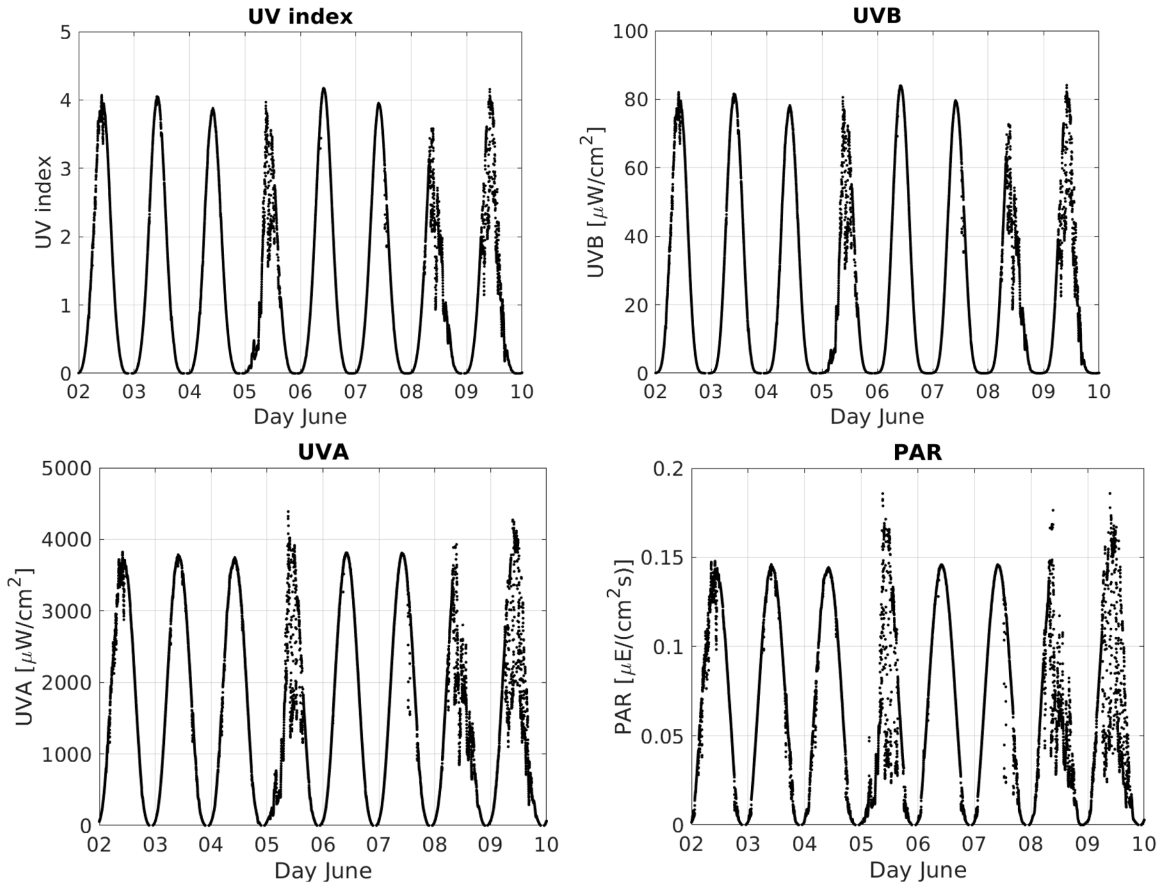

Fig. 8. UV index, UVB, UVA and PAR radiation measured with the GUV radiometer during the campaign week June 2-9, 2021, in Sodankylä.

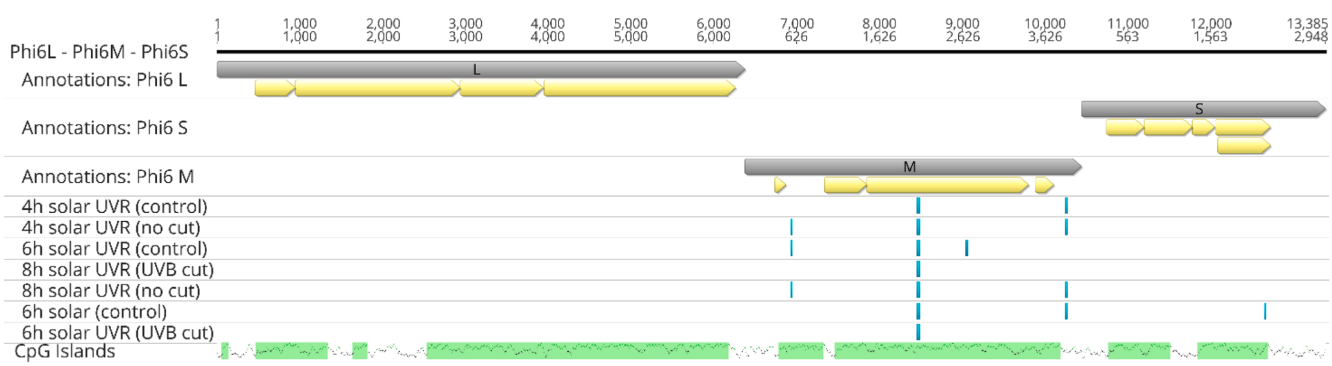

Fig. 9. Deletion-like damages (blue) identified in sequenced Phi6 genomes aligned to Phi6 genome from NCBI database (L, M and S fragments acc. numbers NC_003715.1, NC_003716.1 and NC_003714.1).

before by the US EPA (2020). Lower virus counts on the solar UVA exposed samples was likely due to the UVB filter causing the air to not circulate as well on the petri dish, causing heating, or to UVA effects on virus viability (Bernhard et al., 2023) The effect of UVR on viability was more apparent on the host bacterial strain (Supp. Fig. 9), even though *P. phaseolicola* genome is known to contain fitness determinants conferring among others, tolerance to UV (Pérez-Martinez et al. 2008). According to our findings, bacterial growth was inhibited within a four to five hours period if UVB radiation was present. However, if bacteria were only exposed to the UVA segment of the spectrum, the effects on cell viability remained within confidence intervals. While all genetic damages detected were in non-coding areas of the HB10Y genome, it is possible that they appeared in regulatory sequences, which could explain the growth inhibition. No mutation-like damages were found in the Phi6 genomes exclusive to the UVR exposed samples, most likely due to reasons stated above. However, common deletion-like damages were found in some Phi6 samples, including the controls, indicating that they might have resulted from other environmental stress factors. Additionally, the Phi6 strain in use could have mutated from the sequence used for the comparison during purification, storing and thawing. Most of these damages were found in the M-segment of Phi6, indicating that the M-segment might be more sensitive to variations than other segments. Sequenced virus samples were not passed through a replication cycle, meaning the observed damages cannot be verified as mutations. Still, these findings help us understand what parts of the Phi6 genome are most susceptible to damage. In the host bacteria's genomes, eight possible mutations caused by UVR were identified. Out of these, three produced either cytosine or thymine capable of forming pyrimidine dimers, commonly caused by UVR (Rastogi et al 2010). Bacteria with these mutations were non-growing, indicating that these are weak spots in essential genes.

Our findings suggest that UVR most likely has minimal effect on potential loss-of infectivity of virus aerosols during short-distance transport as tested in this Arctic setup. The solar UVR dose required for significant loss of infectivity would translate into several hours of time-of-flight exposure depending on weather conditions to take effect on Phi6, according to our results. However, in locations with periods of high solar UV activity, the significance of solar UVR on viral aerosols may be significant. The Phi6 solar UVR resilience test results also need to be tested and adapted for virus aerosols instead of dried particles on a surface. However, these tests would require conditions with potential of higher UVR exposure doses during short time of flight for feasible sample collection, which is not available in an Arctic environment. Additionally, other model viruses should be experimented with to understand how different viruses remain infectious in aerosols.

This study also has some potential limitations regarding virus detection and RNA purity. Firstly, BioSamplers have been observed to have reduced ability to collect particles sized <400 nm (Li et al., 2018), suggesting that the actual virus concentrations could be higher than reported here. Additionally, the vortex in the sampler could partially inactivate the collected viruses (Lednicky et al., 2016). Secondly, the purified RNA from Phi6 UV-exposure samples was not optimal (Supp. Table 1), which could result in sequencing errors. However, quality checks on the RNA sequences did not show anything abnormal in sequence quality. Moreover, our findings of no UVR-induced damages in Phi6 genomes aligns with previous studies on Phi6 resilience against UVR, suggesting that RNA purity did not affect the presented results.

We demonstrated that Phi6 remains infectious in outdoor aerosols for at least 50 m downwind, with a potential of even longer distance detection. Even though wind directions were mostly towards our setup, virus-containing aerosols spread not only downwind, but also at least 10 m to both sides from the source. We detected no genomic damages caused by either solar UVR or UVR lamp in Phi6, however, we observed multiple UVR-induced SNPs in HB10Y's genome, some of which could result in cell death.

CRediT authorship contribution statement

Rasmus Malmgren: Writing – review & editing, Writing – original draft, Visualization, Investigation, Formal analysis, Data curation, Conceptualization. **Svetlana Sofieva-Rios:** Writing – review & editing, Writing – original draft, Visualization, Investigation, Formal analysis, Data curation. **Kaisa Lakkala:** Writing – review & editing, Writing – original draft, Visualization, Supervision, Resources, Project administration, Investigation, Funding acquisition, Formal analysis, Data curation, Conceptualization. **Eija Asmi:** Writing – review & editing, Resources, Investigation, Data curation, Conceptualization. **Yan Sun:** Writing – review & editing, Writing – original draft, Visualization, Investigation, Formal analysis, Data curation. **Michael Todt:** Writing – review & editing, Writing – original draft, Visualization, Formal analysis. **Paavo Heikkilä:** Writing – review & editing, Writing – original draft, Visualization, Resources, Formal analysis, Data curation. **Dennis Bamford:** Writing – review & editing, Supervision, Project administration, Methodology, Funding acquisition, Conceptualization. **Martin Romantschuk:** Writing – review & editing, Supervision, Resources, Methodology, Investigation, Funding acquisition, Conceptualization. **Nina Atanasova:** Writing – review & editing, Supervision, Resources, Project administration, Methodology, Investigation, Funding acquisition, Formal analysis, Conceptualization.

Declaration of competing interest

The authors declare that they have no known competing financial interests or personal relationships that could have appeared to influence the work reported in this paper.

Acknowledgements

We thank Helin Veskiväli for excellent technical assistance.

The facilities and expertise of the HiLIFE Biocomplex unit at the University of Helsinki, a member of Instruct-ERIC Centre Finland, FINStruct, and Biocenter Finland are gratefully acknowledged.

Jonathan Duplissy from INAR research institute of University of Helsinki is thanked for providing the filter collector, a valuable measurement device for the campaign.

We thank Markku Ahponen and Juha M. Karhu, Santeri Vehma for technical assistance in Sodankylä and Tuukka Ryynänen in Soilia. We thank Germar Bernhard from Biospherical Instruments Inc. for calibration of the GUV radiometers. We thank Petri Kärhä from Aalto University for the irradiance scale of the UV lamps.

We thank VTT Technical Research Centre of Finland for allowing us to use their Biosampler-aerosol collectors.

We acknowledge the DNA Sequencing and Genomics Laboratory (supported by HiLIFE and Biocenter Finland funding), Institute of Biotechnology, University of Helsinki for sequencing.

The authors wish to acknowledge CSC – IT Center for Science, Finland, for computational resources.

This work was supported by the Academy of Finland COVID-19 Special funding 335681 to N.S.A and the Scientific Advisory Board for Defense (MATINE) Grant No. VN/627/2020-PLM, Business Finland funding for E3, Excellence in Pandemic Response and Enterprise Solutions Co-Innovation project, Academy of Finland CHAMPS project (grant no. 329225) under the CLIHE programme, and Academy of Finland Flagship funding (grant no. 357904)

Open access funded by Helsinki University Library.

Supplementary materials

Supplementary material associated with this article can be found, in the online version, at doi:10.1016/j.envadv.2024.100600.

Data availability

Data will be made available on request.

References

Ariza-Mateos, A., Prieto-Vega, S., Díaz-Toledano, R., Birk, A., Szeto, H., Mena, I., Berzal-Herranz, A., Gómez, J., 2012. RNA self-cleavage activated by ultraviolet light-induced oxidation. Nucleic. Acids. Res. 40 (4), 1748–1766. https://doi.org/10.1093/nar/gkr822.

Au, C.H., Leung, A.Y.H., Kwong, A., Chan, T.L., Ma, E.S.K., 2017. INDELseek: Detection of complex insertions and deletions from next-generation sequencing data. BMC. Genomics. 18 (1), 16. https://doi.org/10.1186/s12864-016-3449-9.

Bamford, D.H., Ojala, P.M., Frilander, M., Walin, L., Bamford, J.K.H., 1995. Isolation, purification, and function of assembly intermediates and subviral particles of bacteriophages PRD1 and σ6. Methods Mole.r Genet. 6, 455–474. https://doi.org/10.1016/S1067-2389(06)80028-2.

Bangiyev, R., Chudaev, M., Schaffner, D.W., Goldman, E., 2021. Higher concentrations of bacterial enveloped virus Phi6 can protect the virus from environmental decay. Appl. Environ. Microbiol. 87 (21), e0137121. https://doi.org/10.1128/AEM.01371-21.

Bernhard, G.H., Madronich, S., Lucas, R.M., Byrne, S.N., Schikowski, T., Neale, R.E., 2023. Linkages between COVID-19, solar UV radiation, and the Montreal Protocol. Photochem. Photobiol. Sci. 22, 991–1009. https://doi.org/10.1007/s43630-023-00373-w.

Bernhard, G., Mayer, B., Seckmeyer, G., Moise, A., 1997. Measurements of spectral solar UV irradiance in tropical-Australia. Atmospheres 102 (D7), 8719–8730. https://doi.org/10.1029/97JD00072.

Bernhard, G., Booth, C.R., Ehramjian, J.C., Quang, V.V.. NSF Polar Programs UV Spectroradiometer Network 2006–2007, Operations Report, 16, Biospherical Instruments Inc., San Diego, available at. https://gml.noaa.gov/grad/antuv/docs/netOps/CHAPTER4.PDF. (Accessed 14 November 2024).

Carvalho, F.R.S., Henriques, D.V., Correia, O., Schmalwieser, A.W., 2021. Potential of Solar UV radiation for inactivation of coronaviridae family estimated from satellite data. Photochem. Photobiol. 97 (1), 213–220. https://doi.org/10.1111/php.13345.

de Courville, C., Cadarette, S.M., Wissinger, E., Alvarez, F.P., 2022. The economic burden of influenza among adults aged 18 to 64: A systematic literature review. Influenza Other Respir. Viruses. 16 (3), 376–385. https://doi.org/10.1111/irv.12963.

Dinoi, A., Feltracco, M., Chirizzi, D., Trabucco, S., Conte, M., Gregoris, E., Barbaro, E., La Bella, G., Ciccarese, G., Belosi, F., La Salandra, G., Gambaro, A., Contini, D., 2022. A review on measurements of SARS-CoV-2 genetic material in air in outdoor and indoor environments: implication for airborne transmission. Sci. Total Environ. 809, 151137. https://doi.org/10.1016/j.scitotenv.2021.151137.

Groulx, N., Urch, B., Duchaine, C., Mubareka, S., Scott, J.A., 2018. The Pollution Particulate Concentrator (PoPCon): A platform to investigate the effects of particulate air pollutants on viral infectivity. Sci. Total Environ. 628–629, 1101–1107. https://doi.org/10.1016/j.scitotenv.2018.02.118.

Guasp, M., Laredo, C., Urra, X., 2020. Higher solar irradiance is associated with a lower incidence of coronavirus disease 2019. Clin. Infectious Dis. 71 (16), 2269–2271. https://doi.org/10.1093/cid/ciaa575.

Koboldt, D.C., Zhang, Q., Larson, D.E., Shen, D., McLellan, M.D., Lin, L., Miller, C.A., Mardis, E.R., Ding, L., Wilson, R.K., 2012. VarScan 2: Somatic mutation and copy number alteration discovery in cancer by exome sequencing. Genome Res. 22 (3), 568–576. https://doi.org/10.1101/gr.129684.111.

Lakkala, K., Arola, A., Heikkilä, A., Kaurola, J., Koskela, T., Kyrö, E., Lindfors, A., Meinander, O., Tanskanen, A., Gröbner, J., Hülsen, G., 2008. Quality assurance of the Brewer spectral UV measurements in Finland. Atmos. Chem. Phys. 8 (13), 3369–3383. https://doi.org/10.5194/acp-8-3369-2008.

Lakkala, K., Aun, M., Sanchez, R., Bernhard, G., Asmi, E., Meinander, O., Nollas, F., Hülsen, G., Karppinen, T., Aaltonen, V., Arola, A., de Leeuw, G., 2020. New continuous total ozone, UV, VIS and PAR measurements at marambio, 64° S, antarctica. Earth. Syst. Sci. Data 12 (2), 947–960. https://doi.org/10.5194/essd-12-947-2020.

Lakkala, K., Suokanerva, H., Karhu, J.M., Aarva, A., Poikonen, A., Karppinen, T., Ahponen, M., Hannula, H.R., Kontu, A., Kyrö, E., 2016. Optical laboratory facilities at the finnish meteorological institute - arctic research centre. Geoscient. Instrument., Methods Data Syst. 5 (2), 315–320. https://doi.org/10.5194/gi-5-315-2016.

Lederberg, J., Lederberg, E.M., 1952. Replica plating and indirect selection of bacterial mutants. J. Bacteriol. 63 (3), 399–406.

Lednicky, J., Pan, M., Loeb, J., Hsieh, H., Eiguren-Fernandez, A., Hering, S., Fan, Z.H., Wu, C.Y., 2016. Highly efficient collection of infectious pandemic influenza H1N1 virus (2009) through laminar-flow water based condensation. Aerosol Sci. Techn. 50 (7), i–iv. https://doi.org/10.1080/02786826.2016.1179254.

Li, J., Leavey, A., Wang, Y., O'Neil, C., Wallace, M.A., Burnham, C.A.D., Boon, A.C., Babcock, H., Biswas, P., 2018. Comparing the performance of 3 bioaerosol samplers for influenza virus. J. Aerosol. Sci. 115, 133–145. https://doi.org/10.1016/j.jaerosci.2017.08.007.

Lubin, D., Jensen, E.H., 1995. Effects of clouds and stratospheric ozone depletion on ultraviolet radiation trends. Nature 377 (6551), 710–713. https://doi.org/10.1038/377710a0.

Ma, B., Linden, Y.S., Gundy, P.M., Gerba, C.P., Sobsey, M.D., Linden, K.G., 2021. Inactivation of coronaviruses and phage Phi6 from irradiation across UVC Wavelengths. Environ. Sci. Technol. Lett. https://doi.org/10.1021/acs.estlett.1c00178 acs.estlett.1c00178.

Mäkelä, J.S., Lakkala, K., Koskela, T., Karppinen, T., Karhu, J.M., Savastiouk, V., Suokanerva, H., Kaurola, J., Arola, A., Lindfors, A.V., Meinander, O., de Leeuw, G., Heikkilä, A., 2016. Data flow of spectral UV measurements at Sodankylä and Jokioinen. Geosci. Instrument., Methods Data Syst. 5 (1), 193–203. https://doi.org/10.5194/gi-5-193-2016.

Mullenders, L.H.F., 2018. Solar UV damage to cellular DNA: from mechanisms to biological effects. Photochem. Photobiolog. Sci. 17 (12), 1842–1852. https://doi.org/10.1039/C8PP00182K.

Oksanen, L., Auvinen, M., Kuula, J., Malmgren, R., Romantschuk, M., Hyvärinen, A., Laitinen, S., Maunula, L., Sanmark, E., Geneid, A., Sofieva, S., Salokas, J., Veskiväli, H., Sironen, T., Grönholm, T., Hellsten, A., Atanasova, N., 2022. Combining Phi6 as a surrogate virus and computational large-eddy simulations to study airborne transmission of SARS-CoV-2 in a restaurant. Indoor. Air. 32 (11), e13165. https://doi.org/10.1111/ina.13165.

Pérez-Martínez, I., Zhao, Y., Murillo, J., Sundin, G.W., Ramos, C., 2008. Global genomic analysis of pseudomonas savastanoi pv. Savastanoi plasmids. J. Bacteriol. 190 (2), 625–635. https://doi.org/10.1128/jb.01067-07.

Plano, L.M.D., Franco, D., Rizzo, M.G., Zammuto, V., Gugliandolo, C., Silipigni, L., Torrisi, L., Guglielmino, S.P.P., 2021. Role of Phage Capsid in the Resistance to UV-C Radiations. Int. J. Mol. Sci. 22 (7), 7. https://doi.org/10.3390/ijms22073408. Article.

Prjibelski, A., Antipov, D., Meleshko, D., Lapidus, A., Korobeynikov, A., 2020. Using SPAdes De novo assembler. Curr. Protoc. Bioinformatics. 70 (1), e102. https://doi.org/10.1002/cpbi.102.

Qiao, Z., Ye, Y., Chang, P.H., Thirunarayanan, D., Wigginton, K.R., 2018. Nucleic acid photolysis by UV254 and the impact of virus encapsidation. Environ. Sci. Technol. 52 (18), 10408–10415. https://doi.org/10.1021/acs.est.8b02308.

Rastogi, R.P., Richa, U., Kumar, A., Tyagi, M.B., Sinha, R.P., 2010. Molecular mechanisms of ultraviolet radiation-induced DNA damage and repair. J. Nucleic. Acids. 2010, e592980. https://doi.org/10.4061/2010/592980.

Rockey, N.C., Henderson, J.B., Chin, K., Raskin, L., Wigginton, K.R., 2021. Predictive modeling of virus inactivation by UV. Environ. Sci. Technol. 55 (5), 3322–3332. https://doi.org/10.1021/acs.est.0c07814.

Rodriguez, R.A., Bounty, S., Beck, S., Chan, C., McGuire, C., Linden, K.G., 2014. Photoreactivation of bacteriophages after UV disinfection: Role of genome structure and impacts of UV source. Water. Res. 55, 143–149. https://doi.org/10.1016/j.watres.2014.01.065.

Sajadi, M.M., Habibzadeh, P., Vintzileos, A., Shokouhi, S., Miralles-Wilhelm, F., Amoroso, A., 2020. Temperature, humidity, and latitude analysis to estimate potential spread and seasonality of coronavirus disease 2019 (COVID-19). JAMa Netw. Open. 3 (6), e2011834. https://doi.org/10.1001/jamanetworkopen.2020.11834.

Savage, N.J., Krentz, C.E., Könemann, T., Han, T.T., Mainelis, G., Pöhlker, C., Huffman, J. A., 2017. Systematic characterization and fluorescence threshold strategies for the wideband integrated bioaerosol sensor (WIBS) using size-resolved biological and interfering particles. Atmos. Meas. Tech. 10 (11), 4279–4302. https://doi.org/10.5194/amt-10-4279-2017.

Singer, B., 1971. Chemical modification of viral ribonucleic acid: IX. The effect of ultraviolet irradiation on TMV-RNA and other polynucleotides. Virology. 45 (1), 101–107. https://doi.org/10.1016/0042-6822(71)90117-6.

Sofiev, M., Sofieva, S., Palamarchuk, J., Šaulienė, I., Kadantsev, E., Atanasova, N., Fatahi, Y., Kouznetsov, R., Kuula, J., Noreikaite, A., Peltonen, M., Pihlajamäki, T., Saarto, A., Svirskaite, J., Toiviainen, L., Tyuryakov, S., Šukienė, L., Asmi, E., Bamford, D., Karppinen, A., 2022. Bioaerosols in the atmosphere at two sites in Northern Europe in spring 2021: outline of an experimental campaign. Environ. Res. 214, 113798. https://doi.org/10.1016/j.envres.2022.113798.

Torremorell, M., Alonso, C., Davies, P.R., Raynor, P.C., Patnayak, D., Torchetti, M., McCluskey, B., 2016. Investigation into the airborne dissemination of h5n2 highly pathogenic avian influenza virus during the 2015 spring outbreaks in the Midwestern United States. Avian Dis. 60 (3), 637–643. https://doi.org/10.1637/11395-021816-Reg.1.

Tseng, C.C., Li, C.S., 2005. Collection efficiencies of aerosol samplers for virus-containing aerosols. J. Aerosol. Sci. 36 (5), 593–607. https://doi.org/10.1016/j.jaerosci.2004.12.004.

Turgeon, N., Toulouse, M.J., Martel, B., Moineau, S., Duchaine, C., 2014. Comparison of five bacteriophages as models for viral aerosol studies. Appl. Environ. Microbiol. 80 (14), 4242–4250. https://doi.org/10.1128/AEM.00767-14.

United Stated Environmental Protection Agency (US EPA). (2020). *Results for SARS-CoV-2 surface disinfection with UV-November 10, 2020* [Reports and Assessments]. https://www.epa.gov/emergency-response-research/results-sars-cov-2-surface-disinfection-uv-november-10-2020.

Vidaver, A.K., Koski, R.K., Van Etten, J.L., 1973. Bacteriophage φ6: A lipid-containing virus of *pseudomonas phaseolicola*. J. Virol. 11 (5), 799–805. https://doi.org/10.1128/jvi.11.5.799-805.1973.

Weyersberg, L., Klemens, E., Buehler, J., Vatter, P., Hessling, M., 2022. UVC, UVB and UVA susceptibility of Phi6 and its suitability as a SARS-CoV-2 surrogate. AIMS. Microbiol. 8 (3), 278–291. https://doi.org/10.3934/microbiol.2022020.

World Health Organization (WHO). (2023). *Influenza (Seasonal)*. https://www.who.int/news-room/fact-sheets/detail/influenza-(seasonal).

World Health Organization (WHO). (2024a, a). *COVID-19 cases | WHO COVID-19 dashboard*. Datadot. https://data.who.int/dashboards/covid19/cases.

World Health Organization (WHO). (2024b, b). *Respiratory syncytial virus (RSV) disease*. https://www.who.int/teams/health-product-policy-and-standards/standards-and-specifications/vaccine-standardization/respiratory-syncytial-virus-disease.